JOURNAL OF APPLIED ELECTROCHEMISTRY 26 (1996) 1267–1272

Changes in cathode catalyst structure and activity in phosphoric acid fuel cell operation

T. MAOKA, T. KITAI, N. SEGAWA, M. UENO

Heavy Apparatus Engineering Laboratory, Toshiba Corporation, 2-1 Ukishima-cho, Kawasaki-ku, Kawasaki, 210 Japan

Received 20 September 1995; revised 1 May 1996

Changes in the cathode catalyst structure and activity obtained from a small size phosphoric acid fuel cell (PAFC) operated for various times up to 12 000 h, were examined. It was confirmed that the platinum surface oxide reduction potential in cyclic voltammograms (CV) shifted in the positive direction with cell operation. This may be one of the manifestations of the activity enhancement for the oxygen reduction reaction (ORR). It was assumed that this activity increase for the ORR was caused by an increase in the surface roughness, due to the dissolution of the alloyed base metals. Changes in the platinum chemical state of the alloy surface, from PtO to Pt, and growth of the Pt (1 1 0) plane would also contribute to this effect.

1. Introduction

Platinum alloy supported on carbon is used as a PAFC cathode catalyst. The alloy components are usually transition metals or refractory metals in groups IV, V, VI, VII and VIII, such as Ti, V, Cr, Mn, Fe, Co and Ni. These catalysts have a higher catalystic activity for ORR than that of a nonalloyed catalyst [1–3]. Cells using these alloy catalysts exhibit high performance from the initial stage of operation. Moreover, the performance decay rate is smaller than that for a cell using a nonalloyed catalyst [4–9].

Clarification of the mechanism of the high catalytic activity of these alloyed catalysts would facilitate the design of a high performance and long life cell. It is known that the alloyed base metals undergo considerable dissolution in the early stage of cell operation [10]. However, after that time, the cell still exhibits better performance than a cell using a nonalloyed catalyst. This phenomenon is of great interest.

In this paper we report the change in the cathode catalyst structure and surface properties of a PAFC catalyst with operation.

2. Previous studies

The mechanism of the high catalystic activity of alloy catalysts for ORR has been studied by many researchers. Excellent review articles have been written on this subject [3–11]. Catalytic activity is explained with reference to structural and electronic properties of the alloy catalyst. Jalan and Taylor [12] reported the importance of the interatomic spacing in the catalytic reduction of oxygen in phosphoric acid. They showed that the specific activity for oxygen reduction increased with a decrease in the Pt–Pt interatomic distance for the alloyed catalyst. We recognize this result as one of the manifestations of the so-called 'volcano relationships' [13]. However, Glass *et al.* [14] insisted that decreased lattice spacing did not correlate with an increase in ORR activity and, moreover, that the atomic ordering in low Cr-content specimens was found to generally promote catalytic activity.

To clarify the role of the alloy metals and their chemical nature at the electrode surface, photoelectron spectroscopic studies, combined with the usual electrochemical techniques, have been implemented by many investigators for the systems Pt/Cr [15–21], Pt/Co [22, 23], Pt/Ti [24], Pt/Fe [25] etc. Daube *et al.* [15] showed that alloyed Cr promotes the oxidation of Pt to Pt^{4+}, leaving a porous platinum electrode with increased electrochemical hydrogen adsorption capacity.

The creation of porous surface structures has been suggested by many other researchers. In a recent patent, it is claimed that elemental gallium is effective for creating a porous structure [9]. Recently, Kim *et al.* [26] confirmed that the mass activity could be enhanced substantially when surface roughening of the catalyst surface occurred while retaining a small metal particle size.

Beard and Ross Jr [23, 24] prepared carbon-supported Pt–Co and Pt–Ti alloys and verified the formation of an ordered alloy of the Pt_3M type by observations of the superlattice line in the XRD pattern. The activity test showed that the most highly alloyed catalysts were not significantly more active than pure Pt, but that the loss of the alloyed metal was the lowest in catalysts which were most alloyed.

0021-891X

Watanabe *et al.* [27] studied the activity and stability of ordered and disordered Co–Pt alloys for PAFC. The ordered alloy exhibited higher activity for ORR than the disordered alloy before the corrosion test but showed less activity after the corrosion test. The authors concluded that the disordered alloy is preferable to the ordered alloy from the viewpoint of stability of both structure and electrocatalytic activity. The high catalytic activity of an ordered alloy was also shown in a recent report by Cho *et al.* [28].

Mukerjee and Srinivasan [29] examined the enhanced electrocatalysis of oxygen reduction on platinum alloys in proton exchange membrane fuel cells. They concluded that the enhanced activity originates primarily as a result of changes in the lattice structure due to alloying and the unique environment of the supported catalyst in the 3.5 ~7.5 nm particle size range.

They also showed that the enhanced electrocatalysis can be rationalized on the basis of interplay between electronic and geometric factors by *in situ* XANES and EXAFS investigation [30].

New and important results were reported by Allen *et al.* [31] on analysing the EXAFS (extended X-ray absorption fine structure) spectra of various platinum alloy catalysts supported on carbon. They found an absence of transition metal coordination to the platinum atoms and proposed that the electrocatalyst consists of essentially three domains: a platinum metal phase, a quasimetallic Pt–O surface layer, and a separate transition metal compound phase (carbide or mixed carbide/oxide). They suggested that this separate transition metal-related compound phase indirectly affected catalyst structure and activity. Because both the platinum and transition metal atoms are situated on a conductive carbon support, their redox chemistry should be intimately related. In addition, the possibility of 10% alloying combined with enhanced activity data for the alloyed materials may indicate that a one-to-one alloy is not a particularly unique requirement for improved catalyst performance.

As seen above, this subject is so complicated that many mutually related factors such as lattice structure, surface roughness, change in electronic properties etc., are closely involved. Change in catalyst properties with cell operation and the reason for maintenance of the activity after dissolution of the alloyed base metals are not yet clear.

3. Experimental details

The test samples of the catalyst layer were obtained from the cathode of a small single cell (electrode area 25 cm^2) operated for various times up to 12 000 h in a vessel pressurized with 8.4 atm of nitrogen gas. The cells were operated at a constant current density of 0.210 A cm^{-2} at 207 °C. The fuel gas was H_2(80%) + CO_2 (20%) and the oxidant gas was air. The fuel gas was humidified with 60 °C water. The gases were supplied to the cell in excess. The cathode catalyst was Pt–Cr–Ni alloy supported on carbon. The contents of the individual metal components were 10, 1.5 and 1.5 wt%, respectively. The gas diffusion electrodes were made by the ordinary method. The PTFE (polytetrafluoroethylene) content was 40 wt%. The electrodes were baked at 360 °C for 20 min. The time-dependent changes in the metal component in the catalyst layer were examined by ICP. (ICP-5000, Shimazu). A fresh electrode was used in each experiment. The cell operation was stopped at various times, and the cathode was analysed using XRD, XPS and CV measurement. XRD patterns were obtained with a Rigaku–Denki (model RAD-2B) X-ray diffractometer in the $20° \leqslant 2\theta \leqslant 55°$ range, at 1 ° min^{-1} scan speed. The power source supplied 20 kV, 20 mA. XPS spectra were obtained by ESCA-LAB5 (VG Co., Ltd, England). The X-ray source was an MgK_α line, and the power source supplied 10 kV, 20 mA. The analysis was carried out in the constant analyser energy mode. The test sample was placed in a vacuum chamber of about 10^{-8} Pa. The axis was corrected for Cls at 284.6 eV.

4. Results and discussion

4.1. *Time lapse of the cell performance*

Figure 1 shows the time lapse of the cell performance at constant current density (0.210 A cm^{-2}) using the alloy catalyst as the cathode. The cell voltage was higher than that of the cell using a nonalloyed catalyst as a cathode by 50 ~ 100 mV. The voltage rose considerably within the initial 100 h; then it decreased linearly with log t by 36 mV decade^{-1}. The voltage gain at the initial stage probably reflects the increase in the wettability of the catalyst layer and the latter part, that is, the gradual decline in voltage, reflects the voltage loss caused by catalyst sintering, or flooding of the electrode with electrolye [32].

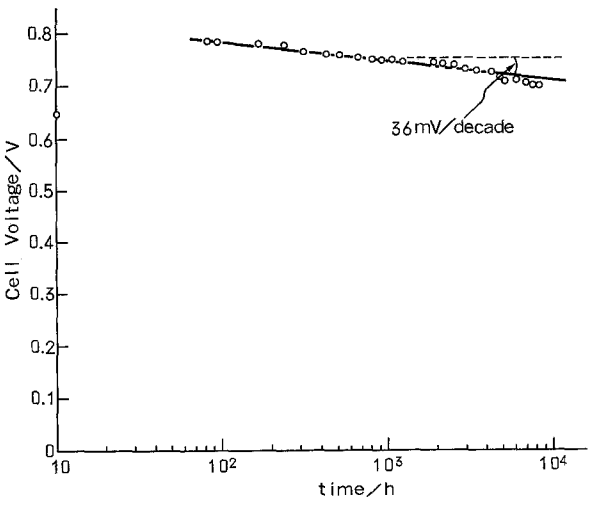

Fig. 1. Cell voltage at fixed currents as a function of time. Conditions: 0.210 A cm^{-2}, 207 °C, 8.4 atm, Pt–Co–Ni/C cathode.

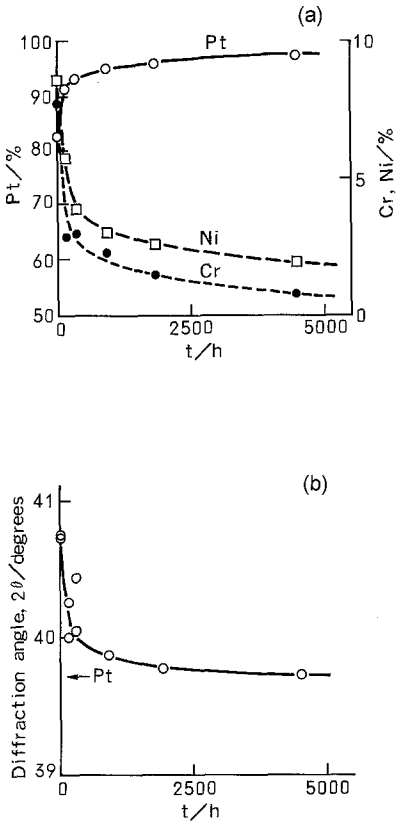

Fig. 2. (a) Changes in the metal component in the cathode catalyst layer; (b) changes in the X-ray diffraction angle of Pt corresponding to (a).

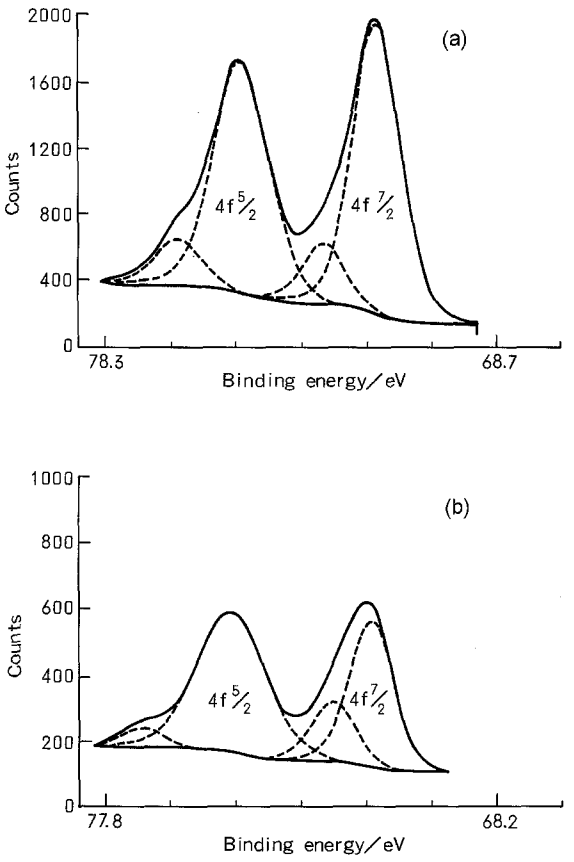

Fig. 3. Pt4f XPS spectra for the cathode catalyst layer: (a) fresh; (b) after 8304 h of cell operation. Key: (—) observed and (– – –) deconvoluted curve; small peak is an asymmetric component of $4f_{5/2}$ and $4f_{7/2}$.

4.2. *Change in the amount of the metal component in the catalyst layer*

Changes in the amount of the metal component in the catalyst layer with cell operation are shown in Fig. 2(a). The amount of alloyed metal, Cr, Ni, decreased steeply within the initial several hundred hours, then decreased gradually, so that the relative Pt content increased. In this process, it is anticipated that the surface roughness increased because a porous structure was created on the surface. Comparing Fig. 2(a) with Fig. 1, it can be said that the dealloying of the base metals has little effect on the cell performance decay, because the voltage did not change abruptly after the initial several hundred hours. It should be noted that the cell voltage was still maintained at a higher value than that of the cell using a nonalloyed catalyst as a cathode, after considerable dissolution of the base metals.

4.3. *Change in X-ray diffraction angle of Pt*

Corresponding to this change in the amounts of metal components, the X-ray diffraction angle for Pt decreased from 40.8° to 39.8°, as shown in Fig. 2(b), which indicates the structural change from Pt-alloy to pure Pt.

4.4. *Change in XPS spectrum*

The XRD spectrum shows the bulk properties for the catalyst layer. On the other hand, information on the surface properties can also be obtained from XPS.

Comparison of XPS spectra for $Pt4f_{7/2}$, and $4f_{5/2}$ obtained before and after cell operation are shown in Fig. 3. After cell operation, the intensity (counts) decreased to about 1/3 of that for the fresh electrode, and the peak position shifted slightly toward a lower binding energy direction. The time dependent change in the $Pt4f_{7/2}$ binding energy is shown in Fig. 4. The energy decreased gradually, which indicates that the Pt surface state changed from PtO_{ads} to Pt [33] with time. Similar behaviour was also recently observed by Aragane *et al.* [34]. This change would increase the Pt activity for ORR, because it is known that surface-chemisorbed oxygen inhibits the ORR [35].

4.5. *CV change*

The CV data, before and after cell operation, are shown in Fig. 5. After cell operation, the double layer current density (c.d.) and current in the hydrogen region decreased considerably, which indicates surface area loss due to sintering. At the same time, the potential corresponding to the current peak for surface oxide reduction shifted positively. It was 0.765 V at the initial stage and became 0.820 V after 12 000 h of cell operation.

The time-dependent change in this potential shift is shown in Fig. 6. The shift increased gradually and

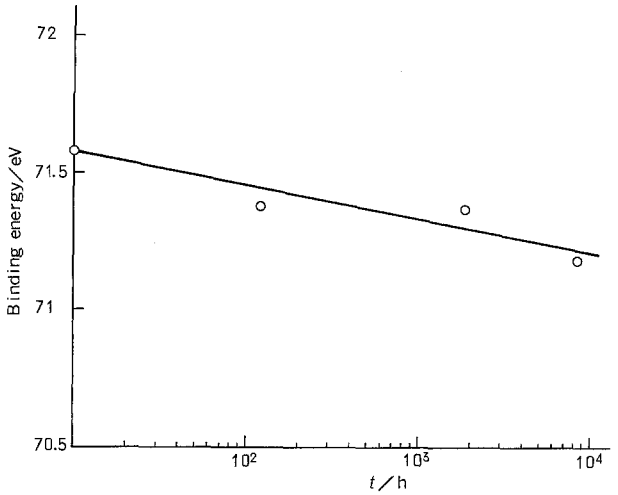

Fig. 4. Change in $Pt4f_{7/2}$ binding energy for the cathode catalyst with cell operation.

after about 2000 h, appeared saturated. This potential shift indicates indirectly that the activity for ORR increased with time.

4.6. *Time-dependent changes in the Pt crystallite structure*

The time-dependent changes in the XRD pattern are shown in Fig. 7. The diffraction peak angles for Pt (1 1 1) shifted to lower values, as indicated in Fig. 2(b), and became sharp.

This indicates that the Pt-alloy changed to pure Pt and shows that crystallite size growth due to sintering has occurred. If a wider diffraction angle range were observed, it could be possible to recognize a small peak appearing at $2\theta = 31.8°$. This peak reflects the Pt diffraction (1 1 0) which is the superlattice line.

Inspection of the higher diffraction angle range indicates the diffraction at the higher plane. These are the Pt (2 0 0) ($2\theta = 46.23°$), Pt (2 2 0) ($2\theta = 67.47°$), and Pt (2 2 2) ($2\theta = 85.71°$). Time-dependent changes in the ratio of the diffraction intensity of these higher planes are shown in Table 1.

Table 1 indicates a time-dependent increase in the (2 2 0) peak ratio. On the other hand, (2 2 2) or (2 0 0) did not change much. This indicates growth for the (2 2 0), that is, the (1 1 0) crystallite plane. This structural change was also supported by the CV. The relative magnitude of the current peak for weakly adsorbed hydrogen grew sharper with cell operation, as shown in Table 2.

Table 2 shows the ratios for the peak c.d. for weakly adsorbed hydrogen (I_w) to those for strongly adsorbed hydrogen (I_s). Because the magnitude of the peak c.d. also reflects the sintering effect, the individual peak c.d. values were divided by the surface area in each case. These values are shown in the last column. I_w increased with time. On the other hand, I_s did not change much or rather decreased.

The current potential profile for well-ordered single crystals, reported by Will [36] and Ross [37], show that weakly adsorbed hydrogen and strongly adsorbed hydrogen are dominant on the (1 1 0) and (1 0 0) planes, respectively. Therefore, this voltammetric behaviour also supports the growth of Pt (1 1 0).

The growth of the Pt (1 1 0) crystallite plane, under PAFC operating conditions, was also observed by Kroen and Stoner [21].

4.7. *Crystallite structure effects on the ORR activity*

Structural effects in electrocatalysis have been frequently discussed in the literature [38]. Crystallite structure effects on the activity for ORR have been

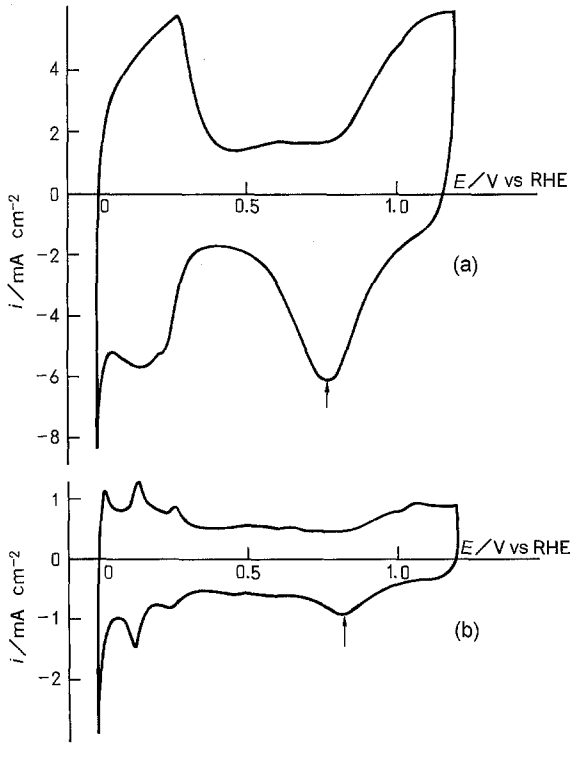

Fig. 5. Cyclic voltammograms of the cathodes before and after cell operation, 10 mV s^{-1}, 25 °C 1 M H_2SO_4: (a) fresh; (b) after 12 000 h. The arrow indicates the current peak for surface oxide reduction.

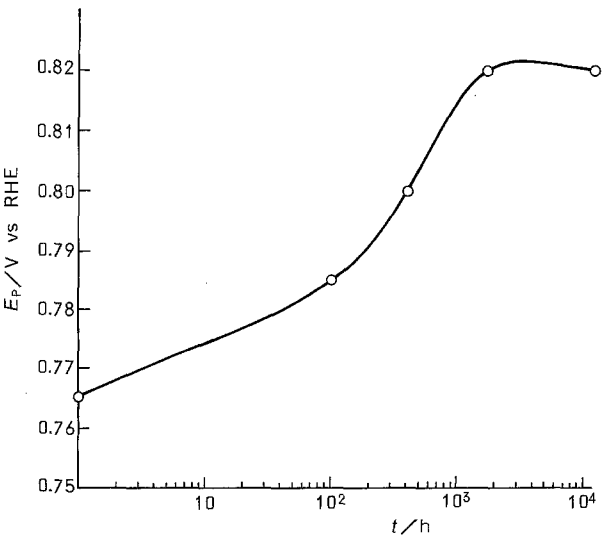

Fig. 6. Change in potential of the surface oxide reduction current peak emerging in CV with cell operation.

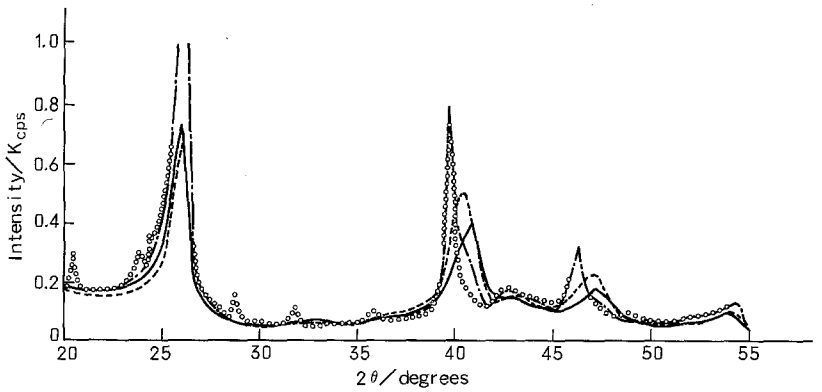

Fig. 7. XRD patterns of the cathode catalyst layers after operation for various times. Key: (—) fresh; (– – –) after 120 h; (– · –) after 1824 h and (OOO) after 8304 h.

reported by several investigators [39–42]. The structure sensitivities were different, depending on the morphology of the test electrode sample. In the case of a single crystal platinum electrode, Tanaka *et al.* [39] found the (1 1 0) > (1 0 0) > (1 1 1) ORR activity order. On the other hand, Ross [40] did not report finding a difference in the activities between (1 1 1) and (1 0 0). In the case of a highly dispersed platinum-supported electrode, Kinoshita [41] observed maximum mass activity for ORR when the (1 0 0) and (1 1 1) surface fractions were maximum. This was attained with a crystallite size of about 3.5 nm. Sattler and Ross [42] suggested that the (1 0 0) and the (1 0 0) vicinal planes are most active for ORR.

As seen above, the effect of the crystallite plane on the activity for ORR is not clear. It seems difficult to discriminate which crystallite plane is more active than the others, especially in the case of a supported catalyst.

4.8. *ORR activity increase mechanism with cell operation*

We assumed that the increases in the ORR activity with cell operation were probably caused by the increase in the surface roughness, due to the dissolution of the alloyed base metals. The change in the chemical state of the platinum on the catalyst surface to metallic Pt and growth of Pt (1 1 0) crystallite plane would also contribute to this phenomenon.

Apart from our results, it seems probable that the redox chemistry of nonalloyed transition metals has a significant influence on the activity enhancement, as pointed out by Allen *et al.* [31].

5. Conclusions

Changes in the structure and activity of the cathode catalyst that were observed in a small PAFC operated for various times were evaluated. It was confirmed that the Pt-alloy catalyst gradually changed to pure Pt with cell operation and that the Pt oxide reduction potential shifted in a more positive direction, which indicates an increase in ORR activity. This activity increase was assumed to result from the increase in surface roughness caused by the dissolution of alloyed base metals and the change in the chemical state of

Table 1. Time dependent changes in the diffraction intensity ratio from a higher plane

	Peak intensity ratio				
Sample	*(200)/(111)*	*(220)/(111)*	*(222)/(111)*	*(200)/(222)*	*(220)/(222)*
Fresh	0.480	0.132	0.163	2.95	0.81
100 h	0.509	0.159	0.113	4.49	1.40
1700 h	0.418	0.152	0.101	4.12	1.50
12000 h	0.450	0.206	0.105	4.27	1.96

Table 2. Time dependent change in the hydrogen adsorption peak current in CV

	Peak current/mA				*Peak current ÷ Pt surface area*/mA cm^{-2}	
Sample	I_w	I_s	I_w/I_s	*Pt surface area*/cm^2	I_w	I_s
Fresh	4.20	2.90	1.45	98	0.043	0.030
100 h	1.45	2.80	0.52	104	0.014	0.027
400 h	2.10	1.15	1.83	46.8	0.045	0.025
1700 h	3.18	1.30	2.45	62.4	0.051	0.021
12000 h	1.75	0.53	3.30	12.5	0.140	0.042

platinum on the crystallite surface to metallic Pt. The structural change in the crystallite perhaps would also contribute to this process.

References

[1] P. N. Ross, Jr, EPRI Report EM-1553 (1980).
[2] J. S. Buchanan, L. Keck, J. Leo, G. A. Hards, N. Scholey, International Fuel Cell Workshop, Tokyo (1989) p. 29.
[3] P. Stonehart, *Ber.Bunsenges. Phys. Chem.* **94** (1990) 913; *J. Appl. Electrochem.* **22** (1992) 995.
[4] V. M. Jalan, *USP 4 202 934* (1980).
[5] D. A. Landsman and F. J. Luczak, *USP 4 316 944* (1982).
[6] F. J. Luczak and D. A. Landsman, *USP 4 447 506* (1984), *USP 4 677 092* (1987), *USP 4 711 829* (1987).
[7] T. Ito, S. Matsuzawa and K. Kato, *USP 4 716 807* (1987).
[8] *Idem*, *USP 4 794 054* (1988).
[9] Chung-Zong Wan, *USP 4 822 699* (1989); F. J. Luczak and D. A. Landsman, *USP 4 806 515* (1989); D. A. Landsman and F. J. Luczak, *USP 4 880 711* (1989).
[10] P. J. Hyde, C. J. Maggiore and S. Srinivasan, *J. Electroanal. Chem.* **168** (1984) 383.
[11] P. L. Antonucci, R. Romeo, M. Minutoli, V. Antonucci and N. Giordano, *Chemical Age of India* **37** (1986) 345.
[12] V. Jalan and E. J. Taylor, *J. Electrochem. Soc.* **130** (1983) 2299.
[13] A. J. Appleby, in 'Modern Aspects of Electrochemistry' (edited by B. E. Conway and J. O'M. Bockris), vol. 9, Plenum Press, New York (1974) p. 453.
[14] J. T. Glass, G. L. Cahen, Jr, G. E. Stoner and E. J. Taylor, *J. Electrochem. Soc.* **134** (1987) 58.
[15] K. A. Daube, M. T. Paffet, S. Gottesfeld and C. T. Campbell, *J. Vac. Sci. Technol.* **A4**(3) (1986) 1617.
[16] S. Gottesfeld, M. T. Paffett and A. Redond, *J. Electroanal Chem.* **205** (1986) 163.
[17] M. T. Paffett, K. A. Daube, S. Gottesfeld and C. T. Campbell, *ibid* **220** (1987) 269.
[18] J. T. Glass, G. L. Cahen Jr, G. E. Stoner, and E. J. Taylor, *J. Electrochem. Soc.* **134** (1987) 58.
[19] J. T. Glass and G. L. Cahen Jr, *ibid.* **135** (1988) 1650.
[20] M. T. Paffett, J. G. Berry and S. Gottesfeld, *ibid.* **135** (1988) 1431.
[21] C. F. Kroen and G. E. Stoner, *Intersociety Energy Conversion Engineering Conference* **25** (1990) 275.
[22] U. Bardi, B. C. Beard and P. N. Ross Jr, *J. Vac Sci. Technol.* **A6**(3) (1988) 665.
[23] B. C. Beard and P. N. Ross Jr, *J. Electrochem. Soc.* **137** (1990) 3368.
[24] B. C. Beard and P. N. Ross Jr, *ibid.* **133** (1986) 1839.
[25] K. T. Kim, J. T. Hwang, Y. G. Kim and J. S. Chung, *ibid.* **140** (1993) 31.
[26] K. T. Kim, Y. G. Kim and J. S. Chung, *ibid.* **142** (1995) 1531.
[27] M. Watanabe, K. Tsurumi, T. Mizukami, T. Nakamura and P. Stonehart, *ibid.* **141** (1994) 2659.
[28] J. Cho, W. Roh and H. Kim, Proceedings of the 2nd International Fuel Cell Conference, **2-01**, 5–8 Feb. (1996) Kobe, Japan, p. 39.
[29] S. Mukerjee and S. Srinivasan, *J. Electroanal. Chem.* **357** (1993) 201.
[30] S. Mukerjee, S. Srinivasan, M. P. Soriaga and J. McBreen, *J. Electrochem. Soc.* **142** (1995) 1409.
[31] P. G. Allen, S. D. Conradson, I. D. Raistrick, S. Gottesfeld, J. Mustre de Leon, M. V. Lovato and P. Stonehart, Proceedings of the Symposium on X-ray Methods in Corrosion and Interfacial Electrochemistry (edited by A. Davenport and J. Gordon), vol. **92-1**, The Electrochemical Society (1992) p. 183.
[32] K. Ito, M. Sakurai, T. Komatsu and H. Miwa, *Denki Kagaku* **57** (1989) 578.
[33] K. S. Kim, N. Winograd, R. E. Davis, *J. Amer. Chem. Soc.* **93** (1971) 6296.
[34] J. Aragane, H. Urushibata and T. Murahashi, *Denki Kagaku* **63** (1995) 642.
[35] V. J. Lukyanycheva, A. V. Yuzhenia, B. J. Lentsner, L. L. Knots, N. A. Shumilova and V. S. Bagotskii, *Elektrokhimiya* **7** (1971) 1287.
[36] F. G. Will, *J. Electrochem. Soc.* **112** (1965) 451.
[37] P. N. Ross, Jr., *Surf. Sci.* **102** (1981) 463.
[38] K. Kinoshita, *in* Proceedings Symposium on Structural Effects in Electrocatalysis and Oxygen Electrochemistry, Electrochemical Society, **92–11** (1991) 307.
[39] A. Tanaka, K. Kanamura, R. Adzic, B. Cahan and E. Yeager, *in* Extended Abstracts, **90–1**, Abstract 667, Spring Meeting of the Electrochemical Society, Montreal, Canada, 6–11 May (1990).
[40] P. N. Ross, Jr., *J. Electrochem. Soc.* **126** (1979) 78.
[41] K. Kinoshita, *ibid.* **137** (1990) 845.
[42] M. L. Sattler and P. N. Ross, *Ultramicroscopy* **20** (1986) 21.